ISSN 1070-3632, Russian Journal of General Chemistry, 2010, Vol. 80, No. 4, pp. 849–856. © Pleiades Publishing, Ltd., 2010.
Original Russian Text © S.V. Zaitseva, O.R. Simonova, O.I. Koifman, 2010, published in Zhurnal Obshchei Khimii, 2010, Vol. 80, No. 4, pp. 688–695.

Structure of Zinc-5,15-di(*o*-methoxyphenyl)octaalkylporphyrines and Their Reaction with Organic Peroxides in the Presence of Pyridine

S. V. Zaitseva, O. R. Simonova, and O. I. Koifman

Institute of Solution Chemistry, Russian Academy of Sciences, Akademicheskaya ul. 1, Ivanovo, 153045 Russia
e–mail: ors@isc–ras.ru

Received June 10, 2009

Abstract—By combined spectral and calculation methods the structure of zinc 5,15-di(*o*-methoxyphenyl)-2,8,12,18 3,7,13,17-octaalkylporphyrinates (**I**, **II**) and their properties in the reaction with organic peroxides with addition of different amounts of pyridine were studied. The reaction of zinc porphyrinates with peroxides in the presence of pyridine leads to destruction of the complex chromophore. Kinetic parameters of the investigated reaction (effective k_{ef} and true k_V rate constants) are obtained. The presence of base in the reaction medium is found to lead to a change in the structure of the zinc porphyrinates and affects the rate of oxidation. By quantum–chemical method PM3 the geometry of the reagents was calculated and the deformation distortions of the reactants molecules and intermediates in the course of the oxidation reaction was demonstrated. The influence of electronic effects of substituents and the degree of deformation of the zinc porphyrinate macrocycle on their redox properties is revealed.

DOI: 10.1134/S1070363210040286

The interest in studying the properties of coordination compounds originates from their ability of molecular recognition of biologically active molecules and the possibility of their application as effective and selective catalysts for redox processes. Previously the results were published of the studies of kinetics and mechanism of oxidation reactions of sterically strained zinc porphyrinates in the medium containing active oxygen in the presence of imidazole and with no additive [1–4]. Much attention was paid to the study of the effect of bases in the reaction medium. In this paper in extension of the understanding of the relationship between the properties of molecular complexes of sterically strained zinc porphyrinates and the structure of macrocyclic ligand and the donor–acceptor properties of nitrogen base, we studied structure of zinc 5,15-di(*o*-methoxyphenyl)-2,3,7,8,12,-13,17,18-octamethylporphyrinate (**I**) and zinc 5,15-di-(*o*-methoxyphenyl)-2,8,12,18-tetramethyl-3,7,13,17-tetrabutylporphyrinate (**II**) and their properties in the reaction with organic peroxides at various concentrations of pyridine in *o*-xylene at 295 K.

The research was carried out by combining spectral methods [5] and quantum–chemical calculations [6–9].

The mechanism of the reaction of zinc porphyrinates **I**, **II** in *o*-xylene with peroxides has been discussed in detail [1–4]. The process takes place on the periphery of the macrocycle and proceeds with the destruction of the chromophore. It is characterized by the reaction rate constants (k_V) 0.0115 and 0.046 s^{-1} mol^{-1} l for compounds (**I**, **II**) and 0.296 and 0.518 s^{-1} mol^{-1} l for their complexes with imidazole (C_{Im} = 4.1× 10^{-3} mol l^{-1}), respectively [1–4].

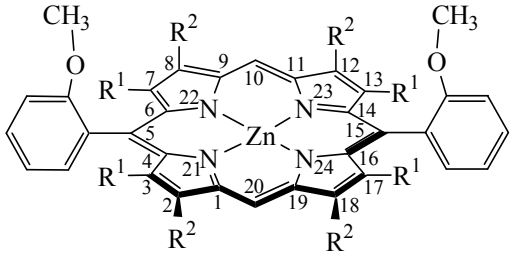

I, $R^1 = R^2 = CH_3$; **II**, $R^1 = CH_3$, $R^2 = C_4H_9$.

The presence of pyridine in the working solution, as in the case of imidazole [3, 4], leads to changes in the structure of macrocyclic compounds and their reactivity. Nature of the reaction does not change (Fig. 1),

in contrast to similar reactions with blocked zinc porphyrinate, where the presence of the base leads to formation of a chlorin complex [10]. The rate–determining step is the formation of intermediates (Py)ZnP(OH)(OR), (Py)ZnP(OH)$_2$, (Py)ZnP(OR)$_2$, (Py)ZnP$^{\bullet}$(OH), (Py)ZnP$^{\bullet}$(OR), (Py)ZnP$^{\bullet}$ for complexes **I** and **II**. Next stages that include destruction of the macrocycle proceed faster.

The variation of concentration of pyridine changes the composition of the reaction mixture and, consequently, the rate of the studied process. Let us consider the conditions when $C_{Py} = 5.0\times10^{-3}$ and 5.0×10^{-2} mol l^{-1}. The first addition of pyridine leads to the formation in the mixture of axial complex (Py)ZnP (**I**, **II**) (Fig. 2a) [11, 12], but its concentration is much less than the initial concentration of zinc porphyrinate. The increase in Py to 5.0×10^{-2} mol l^{-1} results in the change of the ratio of components, that becomes: C_{ZnP} (**I**, **II**) << C_{Py}ZnP (**I**, **II**) (Fig. 2b). In both cases, the rate constant is the overall value characterizing the process which simultaneous participation of zinc porphyrinate **I**, **II** and the respective axial complex. The content of pyridine in the mixture of reagents 4.14 mol l^{-1} leads to instant conversion of all zinc porphyrinate into the axial complex [11, 12], as evidenced by changes in the electronic absorption spectra of metalloporphyrine (Fig. 2c). In this case, the redox reaction proceeds with the participation of the complex (Py)ZnP (**I**, **II**) only.

The values of effective rate constants of the formal first order found for the different initial concentrations of zinc porphyrinate **I**, **II** are listed in Table 1. By processing the linear dependence (1) (Fig. 3) by the least-squares method the order of the reaction on the complex (n) and the true value of a constant rate were estimated. For all three cases $n \approx 1$.

$$\log k_{ef} = \log k_V + n \log [\text{complex}]. \quad (1)$$

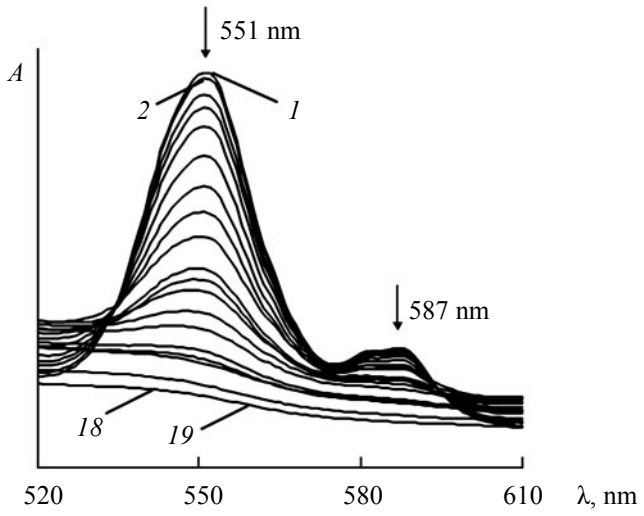

Fig. 1. Changes in electron absorption spectra of ZnP (**II**) in the course of the redox reaction in *o*-xylene ($C_{peroxide}$ = 1.9×10^{-6} mol l^{-1}) at 295 K in the presence of pyridine (C_{Py} = 4.14 mol l^{-1}, $C_{ZnP} = 3.42\times10^{-5}$ mol l^{-1}; *t*, s: (*1*) 0, (*2–18*) intermediate points, and (*19*) 12120.

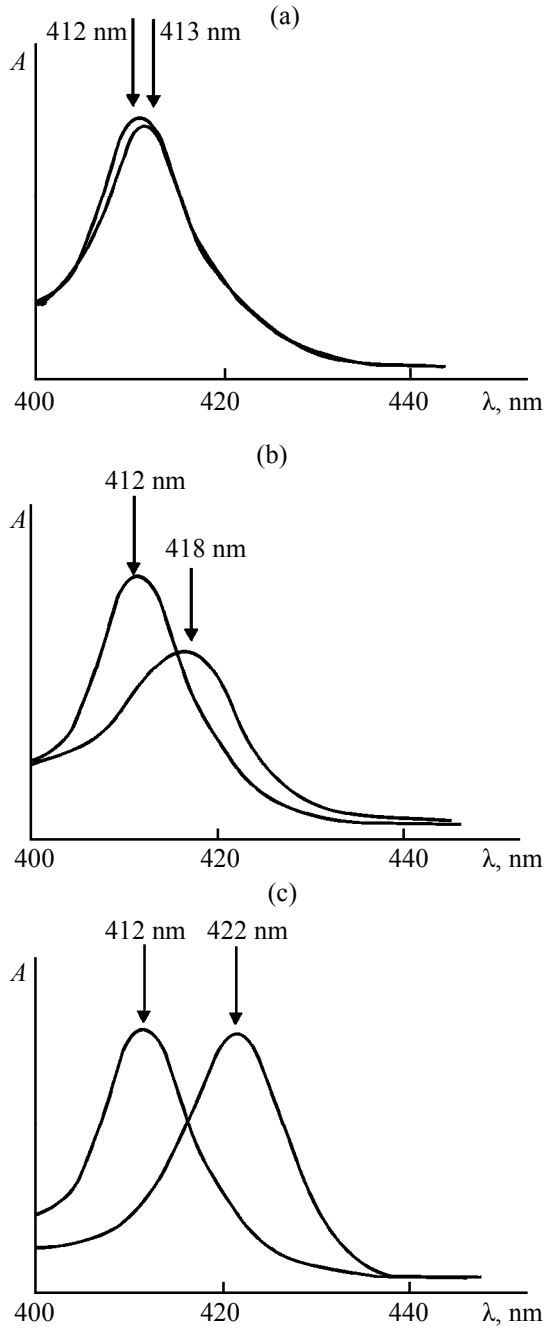

Fig. 2. Changes in electron absorption spectra of ZnP (**II**) with the variation of the concentration of pyridine: (a) Py = 5.0×10^{-3} mol l^{-1}, (b) $C_{Py} = 5.0\times10^{-2}$ mol l^{-1}, and (c) C_{Py} = 4.14 mol l^{-1}.

When Py = 5.0×10^{-3} and 5.0×10^{-2} mol l^{-1} the reaction is described by the scheme:

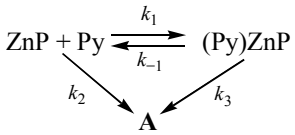

where **A** denotes the products of decomposition.

The reaction rate equation has the form:

$$dC_{\mathbf{A}}/dt = k_2[\text{ZnP}]\,[\text{peroxide}] + k_3[(\text{Py})\text{ZnP}][\text{peroxide}]. \quad (2)$$

Using the equation for the equilibrium constants (equilibrium step in the scheme), we express the concentration of (Py)ZnP:

$$[(\text{Py})\text{ZnP}] = K_{eq}[\text{ZnP}][\text{Py}]. \quad (3)$$

Substituting Eq. (3) into Eq. (2) we get:

$$dC_{\mathbf{A}}/dt = k_2[\text{ZnP}]\,[\text{peroxide}] + k_3K_{eq}[\text{ZnP}][\text{Py}][\text{peroxide}]$$
$$= [\text{ZnP}][\text{peroxide}](k_2 + k_3K_{eq}[\text{Py}]). \quad (4)$$

As a result of research we found the overall constant $k_V = k_2 + k_3K_{eq}$ [Py] (Table 1).

For the reaction involving (Py)ZnP only (Py = 4.14 mol l^{-1}), the equation for the reaction rate becomes:

$$(\text{Py})\text{ZnP} \xrightarrow{k} \mathbf{A},$$

$$-dC_{(\text{Py})\text{ZnP}}/dt = k\text{V}[(\text{Py})\text{ZnP}][\text{peroxide}]. \quad (5)$$

Analysis of the data in Table 1 shows that the rate of redox process involving zinc porphyrinate **II** is higher than the rate of reaction with compound **I**. This is due to the influence of electronic and conformational factors of the macrocycle in the complexes **I**, **II** on their properties. The presence of butyl substituents with the higher electron-releasing properties than the methyl group, and steric strain in the porphyrine ligands in ZnP (**II**) and (Py)ZnP (**II**) leads to a redistribution of electron density in the macrocycle, which contributes to easier rupture of the conjugated bond C_m=C_α and to the formation of a bond at these positions with the peroxide fragments.

The presence of pyridine, as noted above, affects the composition of reagents, alters electronic and geometric structure and steric strain of the macrocyclic compounds. This leads to an increase in the reaction rate (Table 1) compared to the reactions studied in [1, 2]. Nature of the base also affects the redox properties of zinc porphyrinates **I**, **II**. In going from imidazole [3, 4] (with a higher donor number [13]) to pyridine the rate of the studied reaction (Table 1) decreased, and in the case of blocked zinc porphyrinate [10] changed the nature of the process.

Table 1. Kinetic parameters of the reaction of oxidation of ZnP (**I**, **II**) in *o*-xylene in the presence of pyridine ($C_{peroxides}$ = 1.9×10^{-6} mol l^{-1})

$C_{ZnP}\times10^5$, M	Compound **I**			Compound **II**		
	C_{Py}, mol l^{-1}					
	0.005	0.05	4.14	0.005	0.05	4.14
	$k_{ef}\times10^4$, s^{-1}					
12.20			5.601			
11.35			5.210			
8.25			4.077			
7.10	1.311					
6.50	1.250					
5.34	1.110					
4.65					2.790	
4.59		2.851				13.700
4.32				1.238		
4.19				1.198		
4.07						12.460
4.06					2.490	
3.81		2.541				
3.75				1.120		
3.46					2.260	
3.45		2.400				
3.36						11.100
2.83	0.751					
	k_V, s^{-1} mol^{-1} l					
	0.044	0.120	0.743	0.115	0.329	1.466

The effect on the rate of the light components of the source illuminating the reagents is also noteworthy. The exclusion of the ultraviolet spectral region from the total luminous flux leads to 2–6 times decrease in the rate of redox reactions.

Conformational factor of the macrocycles of zinc porphyrinates and their molecular complexes with pyridine, which significantly affects the properties of these compounds, is investigated using quantum–chemical method PM3 [7–9]. The characteristics obtained make it possible to distinguish and estimate the degree of deformation of molecules of the reactants and intermediates of the redox reaction.

The structure of the optimized ZnP (**I**, **II**) molecules is not planar but includes a saddle type

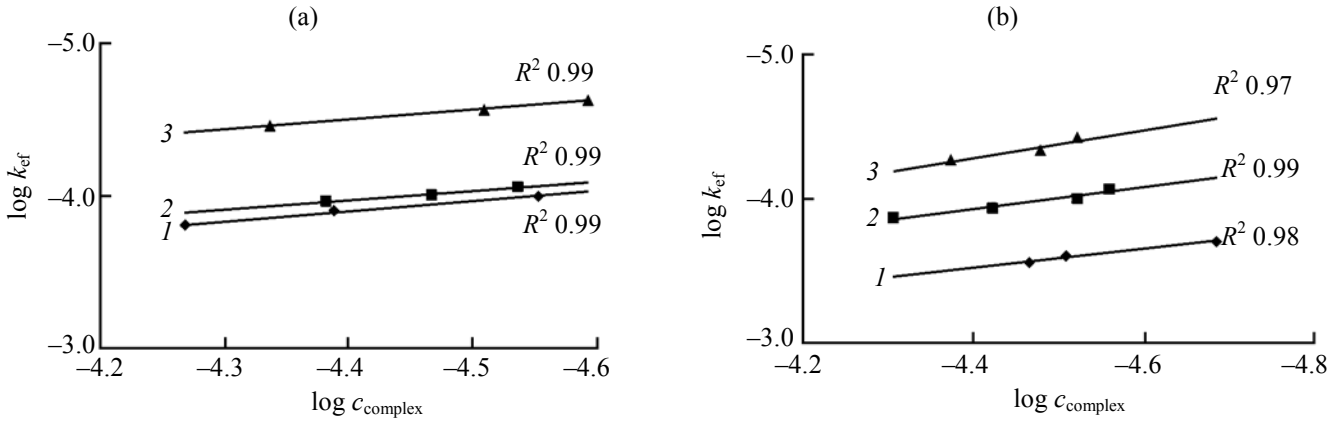

Fig. 3. Dependence of the effective reaction rate constants on the concentration of zinc compound in the presence of pyridine: (a) ZnP (**I**), (b) ZnP (**II**); (*1*) C_{Py} = 4.14 mol l^{-1}, (*2*) $C_{Py} = 5.0\times10^{-2}$ mol l^{-1}, and (*3*) $C_{Py} = 5.0\times10^{-3}$ mol l^{-1}.

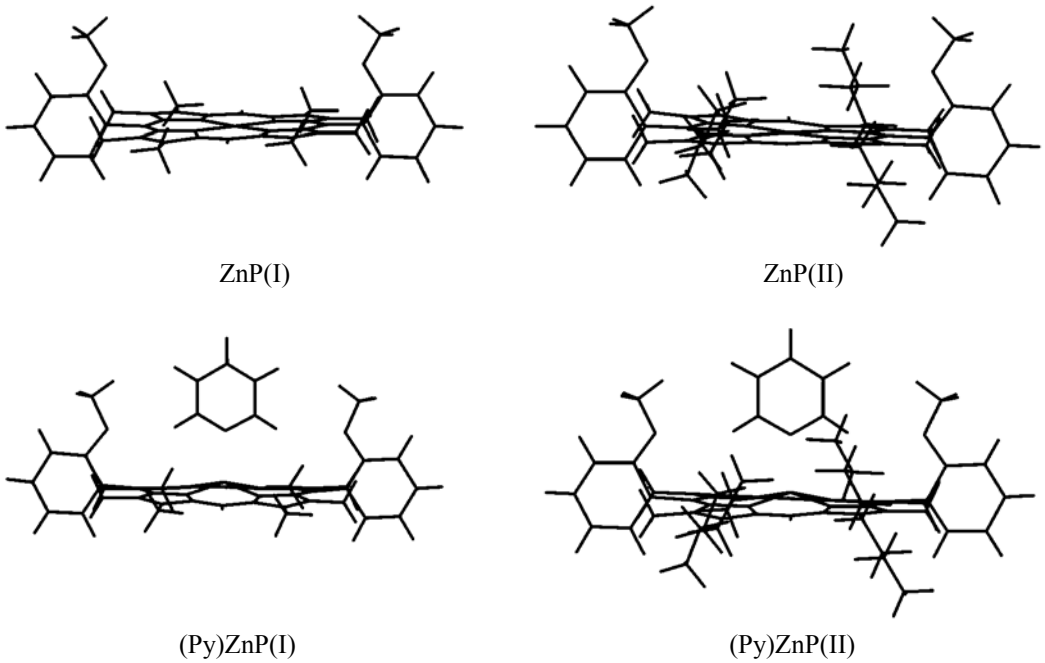

Fig. 4. Structures of ZnP (**I**) and ZnP (**II**) and their axial complexes with pyridine calculated by quantum-chemical method PM3.

strain of macrocycle [1, 2]. Introduction to the reaction mixture of pyridine leads to the formation of complex (Py)ZnP (**I, II**) with a greater steric strain (Fig. 4, Table 2). The type of deformation in this case becomes mixed. In addition to the saddle appear and increase the deformations of dome and groove types (Fig. 5). The coordination center is a pyramid, with a parallelogram in its base (plane N_4). Its perimeter is 11.593 Å and 11.689 Å for the pyridine complexes of zinc porphyrinates **I** and **II**, respectively.

The consideration of the calculated characteristics allows the statement that despite the similarity in the deformations of the compounds (Py)ZnP (**I**) and (Py)ZnP (**II**), the degree of deformation (deviation along the *Z* axis of the backbone atoms of the macrocycle from the average *XY* plane, the value of deviation of the metal atom from the N_4 plane (Ct–Zn), the size of the coordination plane, the bond angles and bond lengths in the methylene bridges, the angles of inclination of pyrrole fragments to the *XY* plane)

differs. Zinc porphyrinate **II** [2] and its molecular complexes are the most sterically strained (Table 2, Figs. 4, 5). With respect to imidazole–containing complexes of **I** and **II** [3, 4] an increase is noted in the strain of their macrocycles in comparison with (Py) ZnP (**I**, **II**) (Fig. 5). It is found that steric strain grows in the seqence: ZnP (**I**, **II**) [1, 2] < (Py)ZnP (**I**, **II**) < (Im)ZnP (**I**, **II**) [3, 4].

Optimized molecular intermediates of the reaction also are not planar, and degree of their deformation exceeds that of the macrocyclic reagents (Table 2, Fig.6). The type of the strain is mixed, but, in contrast to ZnP (**I**, **II**) [1, 2], and (Py)ZnP (**I**, **II**) there is a sharp increase in the saddle and groove deformations (Fig. 6). It is found from the analysis of the calculated data (Table 2, Figs. 5, 6) that the molecules of the

Table 2. Selected geometric characteristics of zinc porphyrinates (**I**, **II**), of their axial complexes with pyridine, and of the reaction intermediates. Numbers of the atoms correspond to IUPAC nomenclature

Complex	$Zn–N_{22}$ $Zn–N_{24}$ Å	$Zn–N_{21}$ $Zn–N_{23}$ Å	$N_{21}–N_{23}$ $N_{22}–N_{24}$ Å	Ct–Zn Å	$Zn–N_L$	P_{N4} Å	$N_{21}ZnN_{24}$ $C_{19}N_{24}Zn$ deg	$C_1C_{20}C_{19}$ $C_9C_{10}C_{11}$ deg	$C_{20}C_{19}C_{18}$ $C_2C_1C_{20}$ deg	$C_{20}C_{19}N_{24}$ $C_{18}C_{19}N_{24}$ deg	$O_1–O_2$[a]
ZnP(I) [1]	2.035	2.084	4.168	0.023		11.647	93.29	126.14	122.45	128.25	10.216
	2.035	2.084	4.069				127.29	126.15	123.67	109.29	
ZnP(II) [2]	2.021	2.061	4.123	0.029		11.609	93.42	125.98	123.03	127.96	10.134
	2.068	2.062	4.088				122.61	126.93	123.31	109.00	
(Py)ZnP(I)	2.076	2.110	4.149	0.378	2.121	11.593	91.86	127.17	122.99	127.95	9.744
	2.107	2.110	4.114				122.38	125.81	125.19	109.05	
$(Py)ZnP(RO)_m(OH)_\alpha$(I)	2.063	2.049	4.104	0.523	2.121	11.575	87.71	119.03	112.42	119.08	9.401
	2.133	2.111	4.064				129.77	125.81	124.13	102.09	
$(Py)ZnP(RO)_\alpha(OH)_m$(I)	2.059	2.124	4.075	0.562	2.106	11.653	87.57	118.48	109.37	114.71	9.546
	2.069	2.158	4.134				127.62	125.91	122.08	102.64	
(Py)ZnP(RO)(RO)(I)	2.063	2.064	4.144	0.555	2.105	11.628	87.07	117.94	109.45	113.68	9.554
	2.138	2.132	4.052				127.08	126.07	123.14	102.75	
(Py)ZnP(HO)(OH)(I)	2.069	2.059	4.136	0.507	2.113	11.634	88.21	119.05	110.34	117.05	9.482
	2.132	2.122	4.067				127.30	126.02	121.50	102.75	
$(Py)ZnP(RO)_m$(I)	2.096	2.101	4.124	0.432	2.097	11.655	89.51	114.52	123.38	126.93	9.481
	2.113	2.110	4.119				125.03	126.14	123.71	109.65	
$(Py)ZnP(OH)_m$(I)	2.096	2.109	4.139	0.423	2.095	11.669	89.78	115.35	122.66	127.59	9.501
	2.110	2.115	4.116				124.75	126.16	122.61	109.69	
$(Py)ZnP(RO)_\alpha$(I)	2.059	2.057	4.134	0.515	2.107	11.631	87.56	126.01	110.97	114.79	9.516
	2.232	2.068	4.065				125.49	126.29	123.56	102.87	
$(Py)ZnP(OH)_\alpha$(I)	2.062	2.061	4.122	0.353	2.105	11.618	87.89	125.67	111.33	114.40	9.491
	2.213	2.072	4.071				125.15	126.29	123.85	102.54	
(Py)ZnP(I)	2.097	2.133	4.204	0.388	2.107	11.769	94.05	138.23	128.25	122.02	9.785
	2.101	2.145	4.125				121.30	126.95	129.62	109.73	
(Py)ZnP(II)	2.084	2.125	4.172	0.385	2.122	11.689	91.24	126.36	123.36	128.11	9.775
	2.093	2.129	4.102				122.26	127.63	123.29	108.53	
$(Py)ZnP(RO)_m(OH)_\alpha$(II)	2.068	2.051	4.161	0.544	2.118	11.608	87.67	120.39	114.52	119.05	9.414
	2.159	2.109	4.116				130.69	126.07	121.53	101.79	
$(Py)ZnP(RO)_\alpha(OH)_m$(II)	2.071	2.057	4.116	0.588	2.109	11.632	87.66	121.33	109.56	116.04	9.466
	2.156	2.118	4.093				129.63	126.22	122.32	102.10	
(Py)ZnP(RO)(RO)(II)	2.0604	2.0519	4.0970	0.574	2.115	11.569	86.61	119.27	111.24	118.11	9.555
	2.1526	2.1093	4.0647				131.08	126.10	123.69	101.82	
(Py)ZnP(HO)(OH)(II)	2.048	2.097	4.329	0.530	2.119	11.976	96.07	108.70	114.23	120.61	9.420
	2.183	2.257	4.096				126.75	125.62	130.51	112.53	

Table 2. (Contd.)

Complex	$Zn–N_{22}$ $Zn–N_{24}$ Å	$Zn–N_{21}$ $Zn–N_{23}$ Å	$N_{21}–N_{23}$ $N_{22}–N_{24}$ Å	Ct–Zn Å	$Zn–N_L$	$P_{N^{2}}$ Å	$N_{21}ZnN_{24}$ $C_{19}N_{24}Zn$ deg	$C_1C_{20}C_{19}$ $C_9C_{10}C_{11}$ deg	$C_{20}C_{19}C_{18}$ $C_2C_1C_{20}$ deg	$C_{20}C_{19}N_{24}$ $C_{18}C_{19}N_{24}$ deg	$O_1–O_2$[a]
(Py)ZnP•$(RO)_m$(II)	2.089	2.099	4.120	0.439	2.097	11.647	89.66	113.22	125.16	124.98	9.480
	2.117	2.114	4.118				123.36	126.71	124.39	109.73	
(Py)ZnP•$(OH)_m$(II)	2.084	2.115	4.161	0.425	2.098	11.682	89.86	115.73	122.87	127.31	9.517
	2.105	2.128	4.103				123.84	126.75	122.98	109.75	
(Py)ZnP•$(RO)_\alpha$(II)	2.060	2.056	4.056	0.566	2.105	11.643	87.42	128.85	111.33	115.35	9.455
	2.248	2.067	4.157				127.15	126.67	123.04	102.28	
(Py)ZnP•$(OH)_\alpha$(II)	2.064	2.062	4.155	0.537	2.107	11.656	88.14	128.22	112.26	115.44	9.484
	2.228	2.071	4.070				126.42	126.73	123.12	102.45	
(Py)ZnP•(II)	2.092	2.141	4.197	0.378	2.106	11.772	94.49	138.96	128.61	121.77	9.788
	2.101	2.134	4.124				120.46	127.60	128.29	109.62	

[a] The distance between the oxygen atoms of OCH_3 groups.

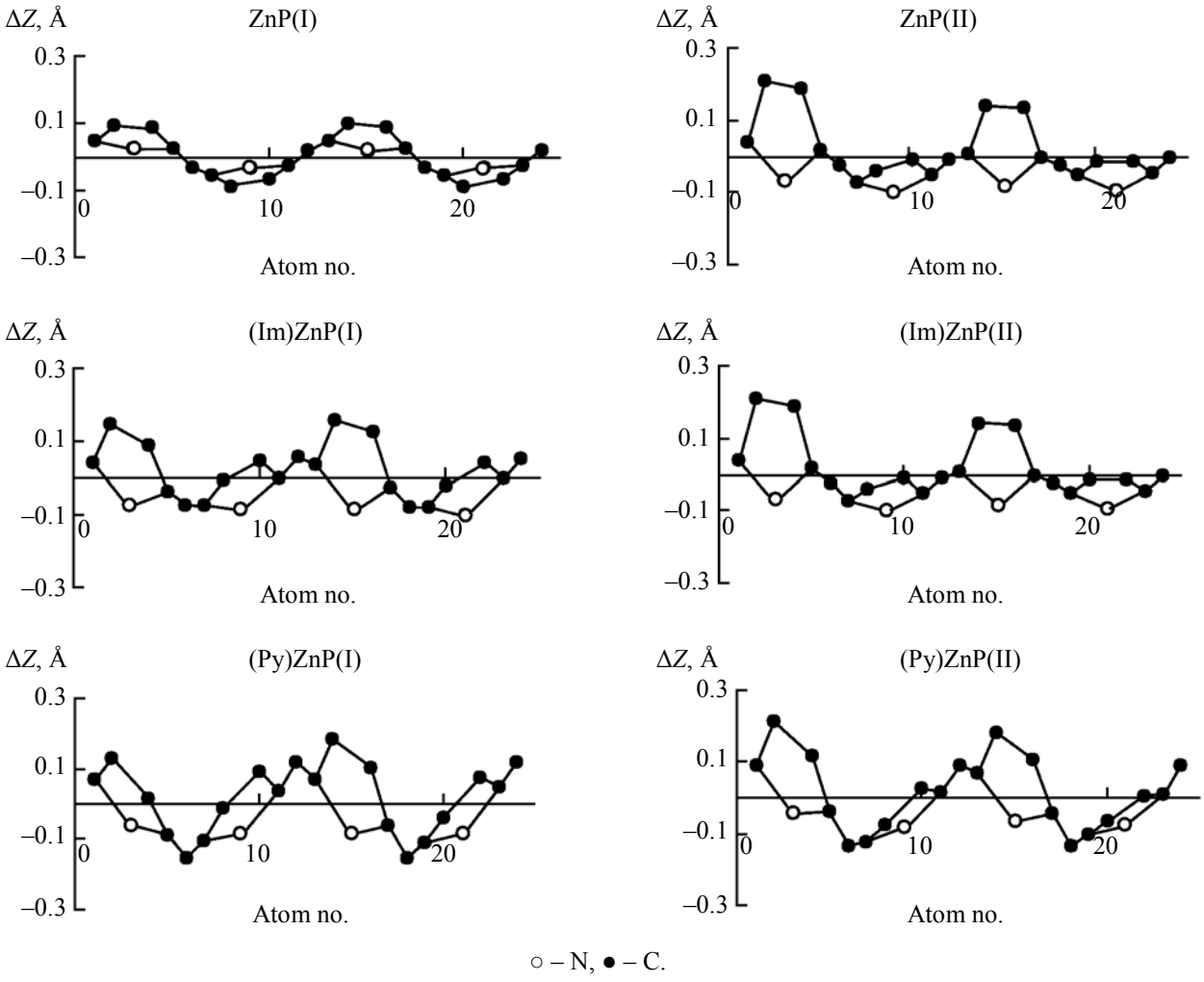

Fig. 5. The deviation from the mean plane of the porphyrin macrocycle backbone atoms (ΔZ) according to the quantum–chemical calculation by PM3 method for ZnP (**I**) and ZnP (**II**) and their axial complexes with imidazole and pyridine.

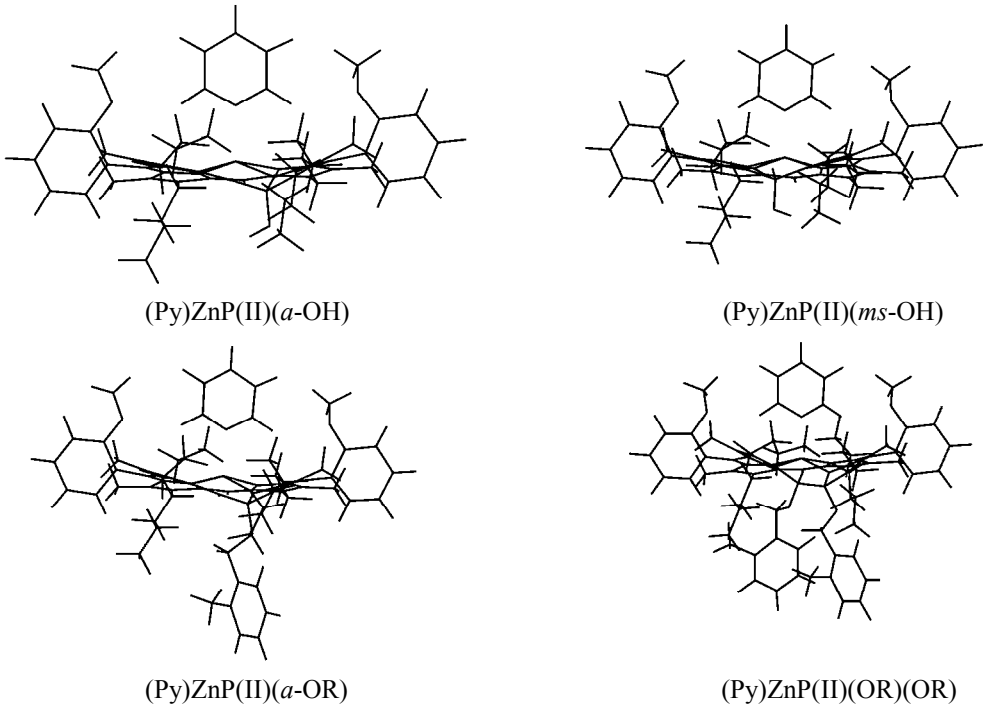

Fig. 6. The structure of some intermediates of oxidation reaction of ZnP (**II**) calculated by quantum-chemical method PM3.

redox reaction intermediates are strongly deformed, are substantially strained and sterically are not very stable. Finally, a cleavage of the macrocycle occurs and the complex is destroyed, that we have observed in the course of experiment.

The difference in the degree of deformation of the investigated now and studied previously [1–4] compounds is reflected in the stability of the reaction intermediates involving these complexes. The series of decrease in stability of intermediates and increase in the reaction rate coincides with the obtained sequence of deformation of the complexes.

On the basis of the material outlined above, we can conclude that the redox properties of zinc porphyrinates **I**, **II** are affected by the nature of the organic bases and by electronic and conformational factors connected with the macrocycle.

EXPERIMENTAL

Synthesis of zinc 5,15-di(*o*-methoxyphenyl)octa-alkylporphyrinates (**I**, **II**) was performed by the standard method [14, 15].

The electron absorption spectra were registered on a Cary 50 instrument at 295 K from the solutions in *o*-xylene. The obtained characteristics [λ_{max}, nm (log ε)] are as follows: for compound **I** 410 (5.18), 538 (4.22), 574 (4.04) for compound **II** 412 (5.22), 541 (4.20), 576 (4.10).

Reaction mixture was irradiated with a moderate pressure mercury lamp TUNGSRAM 20W F33.

Initial concentration of peroxides in *o*-xylene was determined by spectrophotometric method using as an indicator leuco-methylene blue [16]. The method of investigation of the complexation reaction kinetics is described in detail in [17]. Effective rate constant (k_{ef}) of the investigated reaction was determined at the working wavelength λ = 549 nm for compound **I** and 551 nm for compound **II** by measuring a change in the optical density of the solution at regular intervals with analysis according to the formally first–order Eq. (1) maintaining conditions of metalloporphyrin excess:

$$k_{ef} = 1/\tau \ln (C_0/C_\tau), \quad (6)$$

where C_0, C_τ are the concentrations of peroxide at time 0 and τ.

Optimization of the determination of value k_{ef} and of mean square deviations was carried out by the mean-square method using the programs Microsoft Excel and ggh.exe (QB–45) by Guggenheim's method;

both procedures gave the same results. The relative error in determining k_{ef} was 3–5%.

The quantum–chemical calculations were performed at the level of approximation CNDO [18] by the PM3 method [7–9] with complete geometry optimization. A condition for the termination of calculation is the specified gradient 0.0004 kJ mol^{-1} $Å^{-1}$.

ACKNOWLEDGMENTS

This work was supported by the Program for Basic Research of Russian Academy of Sciences "Theoretical and experimental study of the nature of chemical bonds and mechanisms of important chemical reactions and processes" and the Russian Foundation for Basic Research (project no. 09–03–00736–a).

REFERENCES

1. Simonova, O.R., Zaitseva, S.V., and Koifman, O.I., *Zh. Obshch. Khim*., 2008, vol. 78, no. 6, p. 1033.
2. Koifman, O.I. Simonova, O.R., Zdanovich, S.A., and Zaitseva, S.V., Abstract of Papers, *5th Int. Conf. ICPP-5,* Moscow, 2008, p. 424.
3. Simonova, O.R., Zaitseva, S.V., and Koifman, O.I., *Koord. Khim.,* 2009, vol. 35, no. 5, p. 326.
4. Simonova, O.R. and Zaitseva, S.V., *Zh. Obshch. Khim*., 2009, vol. 79, no. 7, p. 1180.
5. Bulatov, M.I. and Kalinkin, I.P. *Prakticheskoe rukovodstvo po fotokolometricheskim i spektrofotometricheskim metodam analiza* (Manual on the Photocolorimetric and Spectrophotometric Methods of Analysis), Leningrad: Khimiya, 1968.
6. Stewart, J.J.P., *J. Comput. Chem*., 1989, vol. 10, no. 2, p. 209.
7. Schidt, M.W., Baldridge, K.K., Boatz, J.A., Elbert, S.T., Gordon, M.S., Jensen, J.H., Koseki, S., Matsunaga, N., Nguyen, K.A., Su, S., Windus, T.L., Dupuis, M., and Montgomeri, J.A., *J. Comput. Chem*., 1993, vol. 14, no. 11, p. 1347.
8. Stewart, J.J.P., *J. Computer-Aided Molecular Desing*, 1990, vol. 4, p. 1.
9. Fletcher, R., *Methods of Optimization*, New York: Wiley, 1980, p. 45.
10. Zaitseva, S.V., Zdanovich, S.A., and Koifman, O. I., *Zh. Obshch. Khim*., 2007, vol. 77, no. 7, p. 1194.
11. Zaitseva, S.V., Zdanovich, S.A., and Koifman, O.I., *Koord. Khim*., 2006, vol. 32, no. 7, p. 504.
12. Zaitseva, S.V., Zdanovich, S.A, and Koifman, O.I., *Russ. J. Phys. Chem*., 2005, vol. 79, no. 1, p. S45.
13. *Tablitsy konstant skorostei i ravnovesii gomoliticheskikh organicheskikh reaktsii* (Tables of Rate and Equilibrium Constants of Hemolytic Reactions in Organic Chemistry), Moscow: VINITI, 1976, vol. 2.
14. Treibs, A. and Haberle, N., *Liebigs Ann. Chem*., 1968, vol. 718, p. 183.
15. Mamardashvili, N.Zh., Semeikin, A.S., and Golubchikov, O.A., *Zh. Org. Khim*., 1993, vol. 29, no. 6, p. 1213.
16. *Comprehensive Organic Chemistry*, Barton, D. and Ollis, W.D., Eds., vol. 2, New York: Pergamon Press, 1979.
17. *Eksperimental'nye metody khimicheskoi kinetiki* (Experimental Methods of Chemical Kinetics), Emanuel', N.M. and Sergeev, G.B., Eds., Moscow: Vysshaya Shkola, 1980.
18. Bersuker, I.B., *Elektronnoe stroenie i svoistva koordinatsionnykh soedinenii* (Electronic Structure and Properties of Coordination Compounds), Leningrad: Khimiya, 1986.